ELSEVIER

Thermochimica Acta 266 (1995) 9–30

thermochimica acta

Relaxational transitions and ergodicity breaking within the fluid state: the sugars fructose and galactose ☆

Jiang Fan *, C. Austen Angell

Department of Chemistry, Arizona State University, Tempe, AZ 85827-1604, USA

Abstract

We describe calorimetric and other studies of time-dependent proceses in some molecular liquids in which there is a higher level of complexity than normally encountered in viscous liquid studies. Best characterized is the sugar D-fructose, which melts to give a liquid which is not in an equilibrium state, and in which slow relaxation processes occur in the liquid far above T_g. These have time scales up to 10 orders of magnitude longer than the shear relaxation time, yet are shown to have an important effect on the liquid viscosity and hence on the value of T_g. Three different heat capacity anomalies are identified, and are assigned to three possible tautomerization equilibria, one of which provides a major contribution to C_p and becomes slow not far below the melting point. The effects of this slow degree of freedom on liquid behaviour are discussed.

Keywords: Ergocity; Fructose; Galactose; Relaxation; Transition

1. Introduction

In most liquids studied to date, the passage from normal low viscosities to the very high viscosity states characteristic of the calorimetric glass transformation range, occurs smoothly. The viscosity, and the related relaxation processes such as dielectric relaxation and spin-lattice relaxation, exhibit monotonic variations which are often well described by the Vogel–Fulcher law. [1, 2] Recently [3], some cases have been discussed in which the passage may be interrupted by first-order transitions with discontinuous changes in viscosity (and also fragility). In the present study, we describe

* Corresponding author.

☆ Dedicated to Hiroshi Suga on the Occasion of his 65th Birthday.

SSDI 0040-6031(95)02551-0

relatively simple systems, the single ring sugars, fructose and galactose, in which the passage may be interrupted by less dramatic, but still significant, changes due to freezing of temperature-dependent tautomer distributions.

Because the ergodicity-breaking in the latter case involves only the conformations of individual molecules, the system remains fluid at lower temperatures. However, its properties at ambient temperature are affected by the rate of passage through the temperature region where distribution freezing occurs because this controls the liquid constitution at the lower temperatures. In this sense, these systems provide new examples of a phenomenon called "superstructuring" when it was first described [4]. The glass-like ergodicity breaking/restoring transitions we observe during cooling/heating in the present liquids could be called, on this basis, "superstructuring transitions" but in this paper we choose instead to simply designate them as EB transitions (EB for ergodicity breaking).

The monosaccharides fructose and galactose both have the formula $C_6H_{12}O_6$. Their structures are depicted, in comparison with other well-studied supercooling molecular liquids, in Fig.1. While in linear chain representation, at least, they appear little different from the six-carbon molecule sorbitol which has been well studied and found to be more or less normal in its behaviour (except for a very broad dielectric relaxation

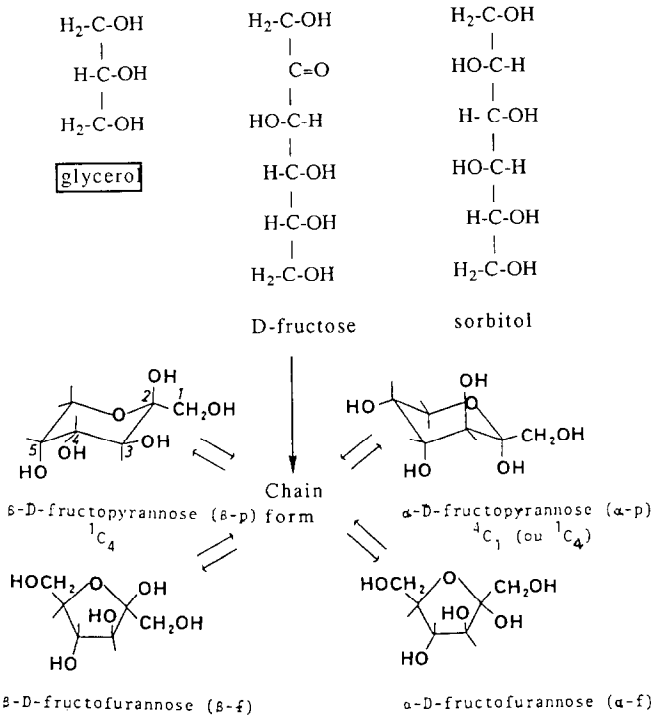

Fig. 1. Molecular structures of the commonly-studied glass formers glycerol and sorbitol, compared with the structure of fructose in chain and ring forms.

spectrum [5], their behavior is quite complex, as we will describe below. This is due mainly to the possibility in these systems of different tautomeric forms of the molecule which can coexist (Fig. 1) but which equilibrate on time scales different from those on which they diffuse and interdiffuse.

Other cases in which slow processes in the high-temperature liquid state have been described, are $CrCl_3 \cdot nH_2O$ [4], liquid sulfur [4], and a borate glass [6]. A number of cases are expected to occur amongst complex aluminosilicates and related compounds, in which the time scale for ordering of Al and Si on the network-forming cation "sub-quasi-lattice" is expected to be much longer than the timescale for viscoelastic relaxation. Indeed it was with such cases in mind that the term "superstructuring" was chosen. To the authors' knowledge, however, there are no measurements detailing how much influence this latter Al–Si ordering process can have on the viscoelastic relaxation time [7].

The cases of greatest interest will, of course, be those in which the slow process has a profound influence on the viscoelastic relaxation. In all likelihood, the best examples of this sort of behavior will be found in the biopolymers of the natural world, but this remains to be established.

In the case of the sugars of the present study, some of the thermal effects associated with freezing of slow degrees of freedom have been observed before [8–10], and have been the center of some controversy which we hope the present article will help settle.

To define terminology, the glass-like transition observed at the lowest temperature, at which the shear relaxation time is $\sim$ 200 s, will be called the glass transition. Subsequent (higher T) "transitions" will, for the sake of convenience, be designated T_1, T_2, etc., in order of their onset temperatures, and will be further designated as EB transitions if it is clear that they become kinetically arrested during cooling.

Finally, in this introduction we stress the complications that may arise from the decomposition (finally caramelization) of sugar melts at "high" temperatures, e.g., at their melting temperatures. The effects of dehydration and other decompositions can intefere with the observations of the effects of the EB transitions, and hence must be avoided.

The decomposition of sugars at temperatures near and above their melting points has been studied thoroughly because the flavoring in foods, and the color ingredients in drinks, mostly come from the caramelization of sugars [11]. These decompositions are various dehydrations and fragmentations (see Ref. [11]). The dehydration of β-D-fructose was studied by Pictet et. al. [12] and Wolfrom et al. [13], and it was found that the dehydration produced various bi-D-fructose anhydrides. The fragmentation process, however, is complex and not well characterized. At least fifteen small-molecule decomposition products have been identified [13]. One of the characteristic consequences of these decompositions is the depression of the glass transition temperature. Details will be given below.

2. Experimental

Because of the importance of the effects of time–temperature histories on the properties of liquid sugars, we have had to prepare the systems for study in different

ways, which we define here. A "partial melt" is one which has been exposed to the melting point of 377.6 K (see below) for less than the time needed to melt the whole sample, hence one which has had minimal opportunity to either decompose or change conformation away from the β-pyranose form of the crystal state. A "fresh melt" is one in which fusion has been completed (so that the mass of liquid phase is now known for quantitative study) but in which the temperature excursion above T_m has been minimized and in which temperature was lowered below 360 K immediately fusion was completed. A "relaxed melt" is one in which the tautomer equilibration has been allowed to occur at a temperature low enough that negligible chemical decomposition is permitted. A "heated-X-hour-at-YK" melt is one which has been subject to the said heating subsequent to being a "fresh melt".

It should be noted here that the melting of a sugar is not a well-defined process because the liquid formed immediately on fusion is not an equilibrium state of the system. This is because the equilibrium state of the liquid, unlike the crystal, is a mixture of tautomers, and the tautomer equilibrium is established on a longer time scale than that of the melting process. We will consider this further in the Discussion section.

The heat capacities have been measured using a Setaram model DSC 121 differential scanning calorimeter using a 10 K min^{-1} scanning rate except where noted otherwise. The accuracy of the instrument was established by reproduction of the literature values for Al_2O_3 [14] and terphenyl [15] to within 2 $\sim$ 3.5% over the temperature ranges 160 and 1000 K respectively.

Enthalpy relaxation in the vicinity of 370 K was determined in the same instrument using an isothermal mode in which thermal fluxes as small as 0.01 mJ s^{-1} were recorded. In these studies, the relaxation at each individual temperature had to be performed with a "fresh" melt.

When the effects of annealing in a high-temperature relaxation range were being probed by post-annealing heat capacity scans, the scans were never taken above 368 K in order to ensure that the results were free from any interference from irreversible processes like dehydration. Evidence that dehydration was avoided is provided below from NMR spectroscopy and is also provided by the near coincidence of the first quenched sample C_p measurements around T_g with the C_p obtained on quenching after completion of all the annealing experiments, as discussed later.

Viscosities were measured with a Brookfield digital viscometer over the range 0.019–10^3 Pa.s). The performance of the viscometer was checked with a standard viscosity oil, and it was found that the experimental error was within 1%. Isothermal viscosity relaxation measurements were obtained in the course of the viscosity measurements.

To obtain samples for the viscosity measurement, the crystal of β-D-fructose was melted at $\sim$ 393 K and, without allowing any further temperature rise, was immediately quenched down to 333 K (this yields a "fresh" melt). The first series of measurements, viscosity vs. T, was carried out from 339.7 to 389.7 K. To study the anomalous high-temperature relaxation, two experiments were then made in which the viscosity was measured as a function of time over some 10^5 seconds at the fixed temperatures 367.2 and 371 K. After this first series, the sample was cooled down to 371 K and held for 8 h so that the structural relaxation in the main EB range could go to completion,

and then the sample was fast-cooled down to 339.7 K. The second series was carried out from 339.7 to 385.2 K, and subsequently series 3 was made during cooling from 385.2 to 329.7 K to check for reversibility. After series 3, the sample was cooled down to room temperature, ~ 296 K, and annealed there for 48 h. Series 4 was then carried out from 335.7 to 371 K during which two weak isothermal viscosity relaxations were recorded.

^{13}C NMR spectra were obtained using a Gemini-300 NMR spectrometer (75.462 MHz, 0.8 acquiring time, 1200 repetitions) with either acetone-d_6 as the internal standard and DMSO as the solvent or D_2O as the solvent and $DCCl_3$ as external standard. The ^{13}C NMR spectra in DMSO were used to determine the relative conformer concentrations in the melts or the crystals, and were acquired immediately after the preparation of the DMSO solution. The interference of solvent DMSO in the determination of the conformer relative concentrations is negligible because equilibrium states among the conformers are only established over several days in this solution according to Nicole et al. [16] and Kuhn and Haber [17]. It was indeed found that it took 3–4 h for any new peaks to become detectable in the ^{13}C NMR spectrum of the solution annealing at room temperature. However, it should be pointed out that Crawford et al. [18] observed rapid tautomerizations of β-D-fructose in DMSO, in obvious contradiction to our own and others' observations. This conflict can probably be explained by the fact that tautomerizations in DMSO are very sensitive to solvent impurities and acids [16, 18].

All ^{13}C NMR spectra using D_2O as solvent were also acquired immediately after the preparation of the solutions. However, these ^{13}C NMR spectra are not suitable for determining the relative conformer concentrations in crystals and melts because, as will be seen, there is little difference in ^{13}C NMR spectra between the solutions made from crystal starting material and crystal solutions made up from fresh melt, which indicates very fast tautomerizations in D_2O solution. Nevertheless, ^{13}C NMR spectra in D_2O solutions are suitable for qualitatively analyzing for decomposition of the melts which might occur during the high-temperature treatment.

The reliability of the conformer relative concentrations derived from the ^{13}C NMR spectrum was tested by the determination of the relative concentration of the conformers of β-D-fructose dissolved in D_2O. The result obtained was: 0.01 α-pyranose:0.73 β-pyranose:0.06 α-furanose:0.19 β-furanose of β-D-fructose in D_2O at 25°C which is in satisfactory agreement with the accepted distribution [8]: 0.02 α-pyranose: 0.7 β-pyranose: 0.05 α-furanose: 0.23 β-furanose in D_2O at 30°C.

3. Results

3.1. ^{13}C NMR *spectra and compositions of tautomerizations in melts*

Fig. 2 shows ^{13}C NMR spectra of DMSO solutions of β-D-fructose made by dissolution of (a) the crystal, (b) the fresh melt, and (c) the heated-2.5 h-at-372 K melt in DMSO at room temperature. Acetone-d_6 was used as the internal standard.

It can be seen that there are many new peaks appearing in the spectrum for solutions of the fresh melt relative to the spectrum of the crystals. This indicates that new

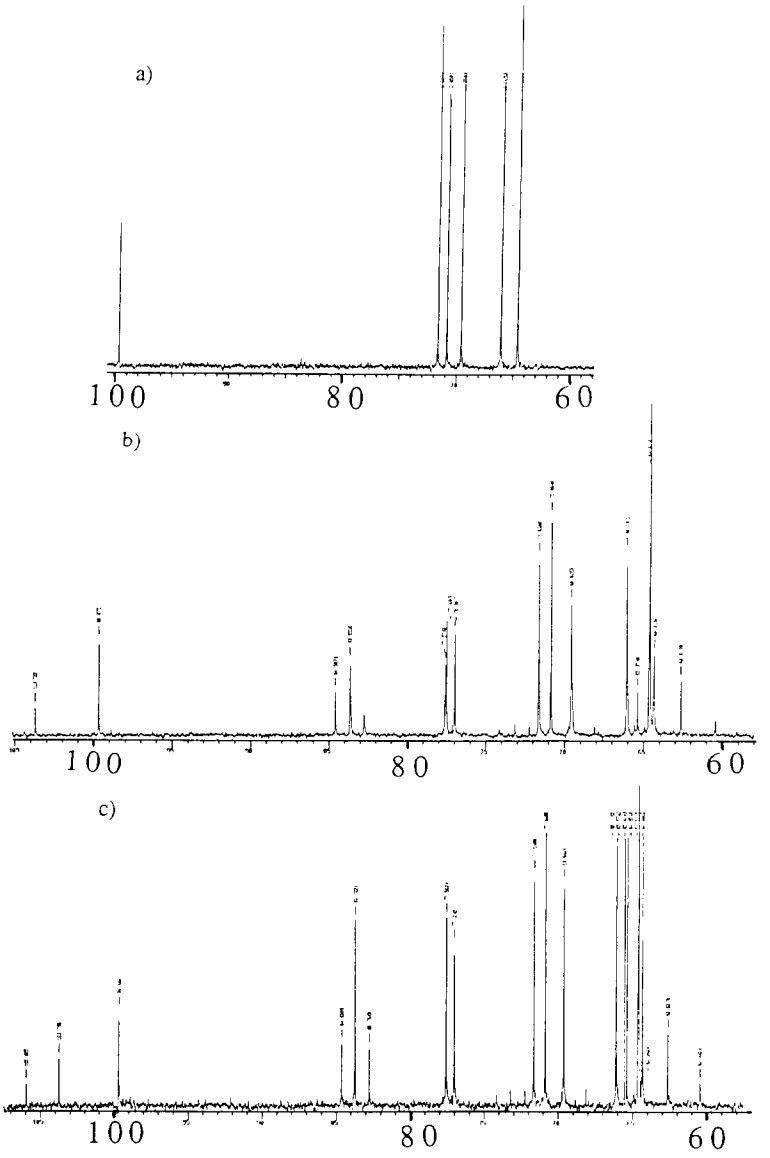

Fig. 2. The ^{13}C NMR spectra showing reasonances in ppm, relative to the standard D-acetone: (a) crystalline fructose; (b) fresh melt (see text); (c) relaxed melt (see text).

conformers are generated in the melting process. The concentrations of the conformers in the melts and crystals determined by ^{13}C NMR spectra in these DMSO solutions according to Horton and Walaszek [19] and Bock and Pederson [20] are listed in Table 1. It is noted that, unlike the melts of β-D-glucose in which there are only

Table 1
The relative conformer concentrations determined by ^{13}C NMR

Substance	State of sample	α-Pyran.%	β-Pyran.%	α-Furan.%	β-Furan.%
β-D-fruct.	Crystal		100		
	Fresh melt	3	60	11	26
	Relaxed[a]	3.5	51	12.5	33
	Fresh, annealed[b]	2.5	61.5	9	27
	Relaxed, annealed[c]	2.6	68.7	7	21.7
α-D-galac.	Crystal	100			
	Fresh melt	33	43	10	14
α-D-gluc.	Crystal	98	2		
	Melt[d]	50	50		
1 α-D-gluc. + 1 β-D-fruct. fresh melt	50% α-D-glucose	45	55		
	50% β-D-fructose	6	43	14	37

[a] Relaxed melt: the fresh melt was annealed at 372 K for 3 h.
[b] The annealed fresh melts: the fresh melt which was annealed at 298 K for 41 h.
[c] Annealed relaxed melt: the relaxed melt was annealed at 298 K for 48 h.
[d] Shallenberger and Birch [12].

pyranose forms, there are significant amounts, of furanose conformers in the melts of β-D-fructose, α-D-galactose, and the mixture of 0.5 β-D-fructose:0.5 α-D-glucose. In addition, for β-D-fructose, it is noted that there are some additional small peaks in the ^{13}C NMR spectrum of the 392 K 1-h-heated melt compared with that of the fresh melt. This means that the composition of the melt was continuously undergoing changes which we associate with decomposition.

As tests for sample purity after study, ^{13}C NMR spectra of β-D-fructose in the following states in D_2O were obtained: (a) the crystal, (b) the fresh melt, (c) the melt annealed at 372 K for 2.5 h or relaxed melt, (d) the melt heated at 374.2 K for 6 h, and (e) the melt annealed at 403.2 K for 2 h. Those of (c) and (e) are shown in Fig. 3.

The spectra of D_2O solutions of the crystal, the fresh melt and the melt annealed at 372 K for 2.5 h, or relaxed melt, have identical peaks indicating that decomposition is negligible in these melts. Note that all peaks of spectra of the crystal, fresh melt and the heated-2.5 h-at-372 K melt can be assigned unambiguously to known tautomers after a −6 ppm correction to the chemical shifts for the external reference has been made [20]. In the melt heated at 374.2 K-6 h, many additional lines are seen though the intensities are not high. These lines are much more pronounced in the 403.2 K–2 h melt, Fig. 3 below, which was evidently seriously decomposed.

Detailed analysis of the decomposition is not possible at this point, and also is not of importance to this paper.

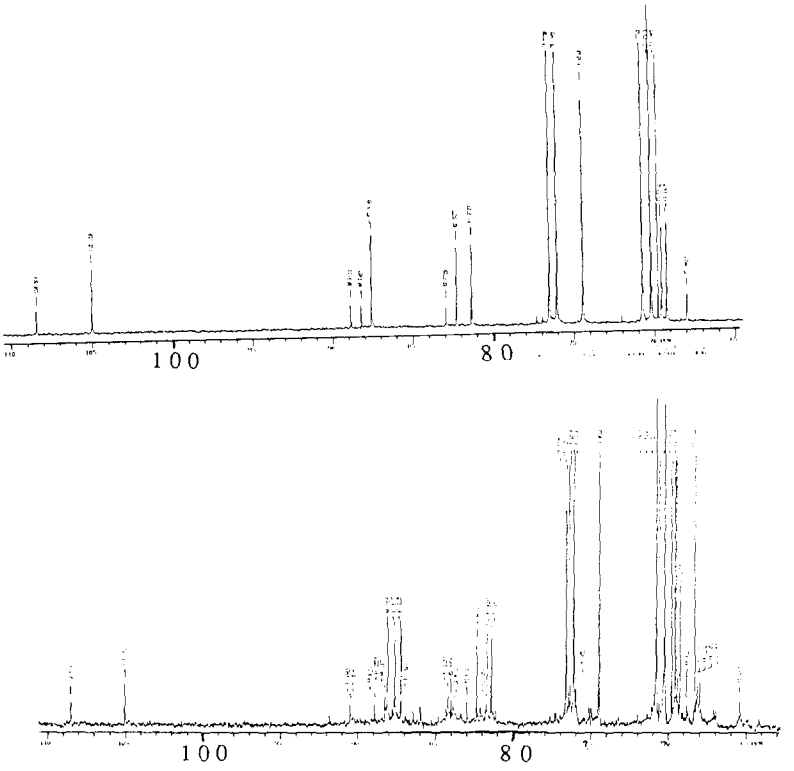

Fig. 3. The ^{13}C NMR spectra for fructose samples showing (upper panel) absence of decomposition products after annealing the melt at 372 K for 2.5 h, and (lower panel) development of many new lines due to decomposition in a melt heated at 403.2 K for 2 h.

3.2. *Heat capacity scans and transitions above* T_g

Fig. 4 shows the heat capacities of β-D-fructose in the following states: (i) the crystal, (ii) quenched partial melts, (iii) quenched fresh melt, and (iv) quenched relaxed melts obtained from the fresh melt having been observed for enthalpy relaxation. It can be seen that the heat capacity of the crystal agrees with the value obtained by Kawaizumi et al. [22] but is ~ 5% higher than that obtained by Finegold et al. [9] Two features are especially to be noted: (i) the glass transition temperature (T_g = ~ 289 K) of the "partial melts" is about 3 K higher than that of the "fresh" melts (T_g = ~ 286 K) and ~ 9 K higher than that of the "relaxed" melt (T_g = 280.2 K), and (ii) there are two anomalies in the C_p of the quenched fresh melt, a weak one starting at 324 K, and a stronger one at 367 K.

For the fresh melt, the larger transition, which will be called hereafter T_2 (at temperature T_{T_2}), is observed at ~ 367 K (see Δ in Fig. 4) and has ΔC_p (77.5 J mol^{-1} K^{-1}) which is ~ 60% of the ΔC_p (133 J mol^{-1} K^{-1}) observed at the glass

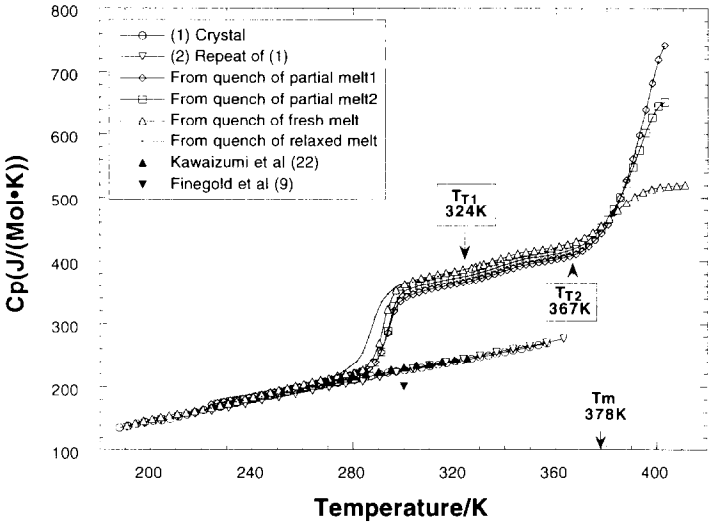

Fig. 4. Heat capacity scans of crystal, partially melted, and fully melted samples of fructose as indicated in the legend. Note that the glassy component of partially melted sample has a higher T_g than the fully melted sample due to retention of a higher fraction of the β-pyranose form. Comparison of the crystal is made with literature values. Note the small step in heat capacity designated T_1 at 324 K and the larger step, designated T_2 at 367 K, in the scan of the fresh melt.

transition temperature 286 K. The smaller transition, T_1 (occurring at T_{T_1}), is observed at $\sim$ 324 K and has ΔC_p (16.6 J mol^{-1} K^{-1}) which is a factor of $\sim$ 4.7 smaller than that of transition 2. T_2 has been reported in previous studies [8–10] but T_1 has not. These effects are also present in the scans of quenched relaxed melts, but T_1 is much weaker.

Fig. 5 shows the effects of annealing the quenched fresh melt at two different temperatures, one below and one above T_g. These annealing effects are kept free from interference by decomposition by stopping measurements at $\sim$ 368 K on each upscan. It is noted that when the β-D-fructose relaxed melts were annealed around 296 K (which is between the glass transition temperature and T_{T_2}), T_g increases by as much as $\sim$ 6 K, see run 6. Also, T_{T_2} decreases as much as $\sim$ 15 K and is smeared out so that T_2 is no longer observable. It is also noted that when the annealing temperature is below the glass transition temperature, the "overshoot" in the glass transition C_p increased in the normal manner while the higher temperature transitions remain unaffected. These annealing effects persist in hydrated melts as will be seen later.

Fig. 6 shows the heat capacities of β-D-fructose melts with the various thermal histories indicated in the figure inset. The numbers give the order in which the run was performed. The same numbering scheme will be used in subsequent figures. Even though partial decomposition (mainly dehydration) complicated the matter in these cases, several features are worth noting as follows.

(a) The relaxation strength of T_2 was accumulated on annealing below T_{T_2}. A big "overshoot" is seen when the melt was annealed between T_g and T_{T_2} (run 3).

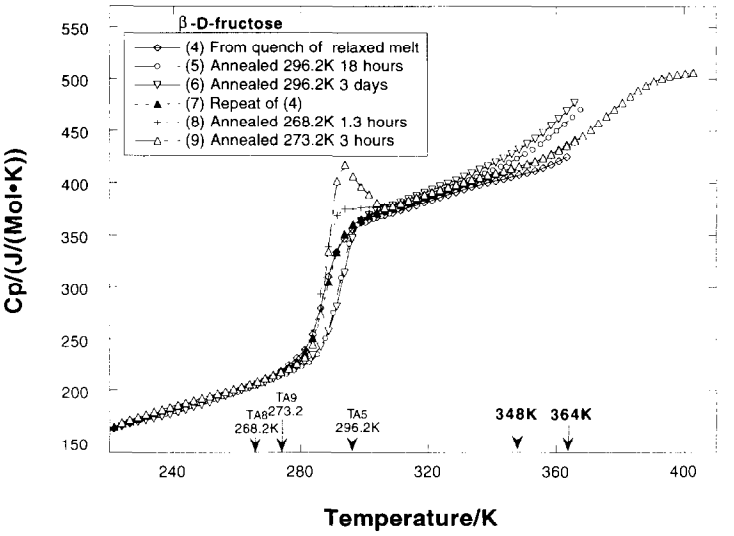

Fig. 5. DSC scans showing effects of annealing of a quenched fresh melt at temperatures above, and also below, T_g.

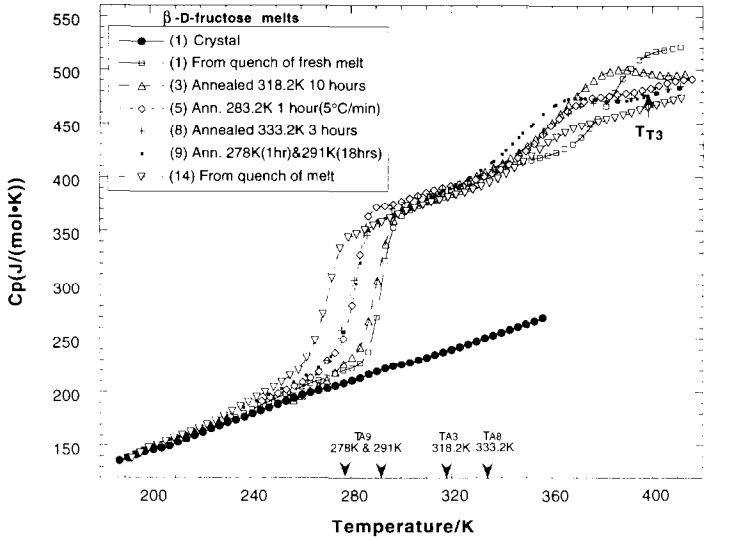

Fig. 6. Comparison of crystal heat capacity with various scans of the liquid and glass after treatment described in the legand. Note the development of an "overshoot" in melts in the old temperatures above T_g.

(b) The sample annealed at 318 K gave the largest overshoot. Annealing at the lower temperature of 278 K gave a smaller overshoot and a lower peak temperature.

(c) $\Delta C_p(T_{T_2})$ at the glass transition at $\sim$ 260–280 K depends strongly on the melt history in the vicinity of 373 $\sim$ 410 K. This is the temperature range in which the

decomposition, particularly dehydration, occurs. For instance, there were decreases of 50 J mol^{-1} K^{-1}, 35 °C and 22 °C in $\Delta C_p(T_{T_2})$, T_{T_2} and T_g respectively after the melts had been repeatedly heated to ~ 410 K (14 times). Thus we confirm Franks' observation [8–10] that, after repeated heating and cooling of the β-D-fructose melt, the prominent higher temperature transition (our T_2) diminshes.

(d) There is a third small transition ($\Delta C_p \approx 7$ J mol^{-1} K^{-1}) at ~ 394 K in the melts which had experienced 5 separate heatings over ~ 410 K. This is seen much more clearly in more slowly scanned samples as in Fig. 8, below. Both the temperature of this third transition (abbreviated hereafter as T_{T_3}) and its ΔC_p decrease whenever the melts experience a heating over 410 K (in the same manner as T_g, $\Delta C_p(T_{T_1})$, T_{T_1} and T_{T_2}). The third transition was not recognized in the fresh melt scanned at 10 K min^{-1} (Fig. 4) because the measurement stopped before it could be observed.

Fig. 7 shows the heat capacities of the melts of β-D-fructose in the vicinity of T_{T_2} obtained with a smaller scanning rate, 3 °C min^{-1}. It can been seen that for the fresh melt, there is a small endothermic (melting-like) peak beginning around 376 K at which the isothermal enthalpy relaxation (see below for detail) was fast. This measurement indicates that some processes in the fresh melt did not have enough time to equilibrate during melting and therefore resumed equilibration (with absorption of some heat) as soon as the temperature reached values at which the processes could proceed significantly during a 3 °C min^{-1} reheating run. It can also be clearly seen in the second run that at ~ 395 K there is a third, also small, EB transition (T_{T_3} = ~ 395 K, $\Delta C_p \approx 10$ J mol^{-1} K^{-1}, i.e., ~ 13% of $\Delta C_p(T_{T_2})$), which confirms the observations in Fig. 6.

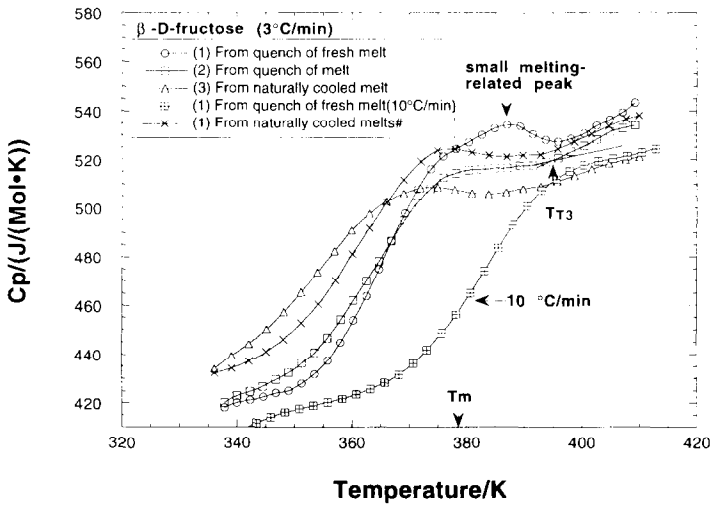

Fig. 7. Slow (3 °C min^{-1}) scans of fructose melts at higher temperatures showing (a) the onset of a small endothermic peak related to processes within the melt which were incomplete at the melting point, and (b) the presence of an additional anomaly designated T_3 at ~ 395 K. Comparison is made with the previous scan made at 10 °C min^{-1}.

Fig. 8. shows the heat capacities of the fresh melts of (i) the binary blends, β-D-fructose and α-D-glucose, (ii) pure α-D-glucose in the vicinity of T_{T_2}, and (iii) some literature values [22]. The insert is $\Delta C_p(T_{T_2})$ in relation to the mole fraction of β-D-fructose. It is particularly to be noted that the liquid melt of glucose also has an anomaly around 360 K which has never been reported before. The addition of glucose results in a more-or-less linear decrease of $\Delta C_p(T_{T_2})$ and small decrease in T_{T_2}.

Fig. 9 shows the heat capacities of α-D-galactose in the following states: (i) the crystal, (ii) the fresh melt, and (iii) the melts with the thermal histories specified on the figure. It can be seen that the heat capacities of the crystal are ~ 5% lower than that obtained by Kawaizumi et al. [22], but ΔC_p, 135.7 J mol^{-1} K^{-1} at T_g (290 K), agrees well with the literature value, 135.2 J mol^{-1} K^{-1} [23]. It can be seen that the α-D-galactose melt has a well-defined transition above T_g ($\Delta C_p \approx 44.5$ J mol^{-1} K^{-1}) at ~ 353 K, as has been described before [9]. However, it also has a very small, less well-defined, EB transition (EBT1) ($\Delta C_p \approx 5$ J mol^{-1} K^{-1}) at ~ 302 K, just above the glass transiton. It is obvious that α-D-galactose melts behave in a similar manner to β-D-fructose melts except for the absence of EBT3 and some quantitative differences such as a smaller ΔC_p at T_{T_2} and smaller annealing effects.

3.3. *Isothermal enthalpy relaxations*

Fig. 10 shows the isothermal enthalpy relaxations of the fresh melts of β-D-fructose at various temperatures. The relaxation process is endothermic (negative heat flux means

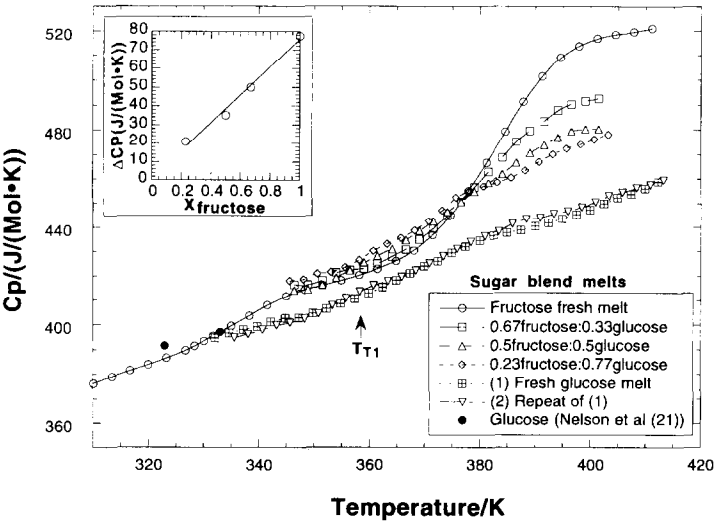

Fig. 8. Heat capacity scans for pure fructose and glucose fresh melts and various blends as indicated in the legand. Comparison is made with literature data for the case of glucose. Attention is drawn to the presence of a small anomaly in the case of glucose which has not been seen before. Insert shows effect of glucose content on the height of the liquid state heat capacity anomaly designated T_2.

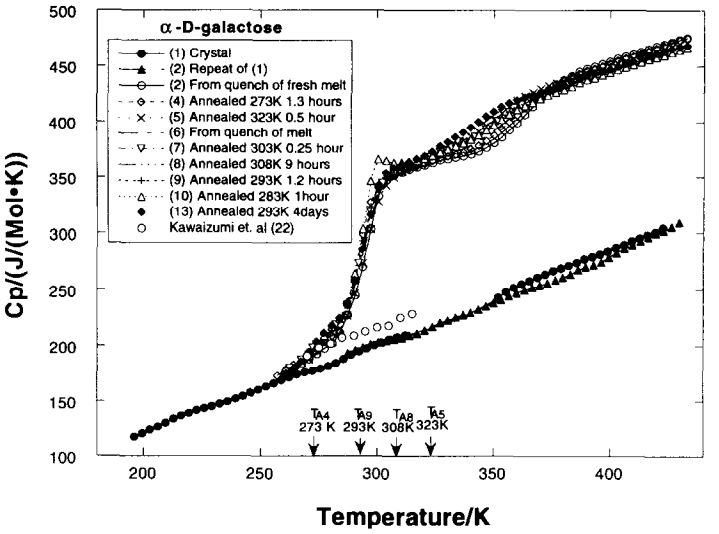

Fig. 9. Scans of the crystalline and liquid states of α-D-galactose following different thermal histories as designated in the legend. Comparison is made with data reported in Ref. [22].

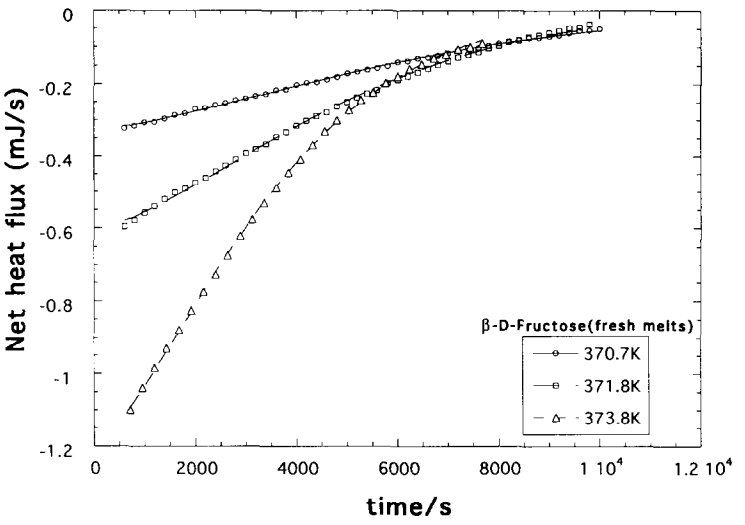

Fig. 10. Isothermal enthalpy relaxation near 370 K in fresh melts of β-D-fructose. Below 370 K, the relaxation becomes almost unobservable.

endothermic) with a small amount of heat being absorbed, 13.9 kJ mol^{-1} at 373.8 K (compare $\Delta H_f = 29.81$ kJ mol^{-1} at $T_f = 378$ K). The isotehrmal relaxation is not a simple exponential relaxation. The *magnitude* of the enthalpy relaxation decreased rapidly with decrease in temperature, such that the enthalpy relaxation could not be

detected below about 369 K. The enthalpy relaxation could be obtained only in fresh melts and could not be observed again even if the melt was annealed at room temperature for days. The ^{13}C NMR spectrum of the relaxed melt (Fig. 2) established that decomposition was negligible during the enthalpy relaxation measurement. (Attempts were made to observe isothermal enthalpy effects due to decomposition by raising the temperature to 393 K at which the colorless melts become yellow, but no effect could be observed.)

3.4. *Viscosities and isothermal relaxations of viscosity*

The viscosities of β-D-fructose melts are shown in Fig. 11. It can be seen that our viscosity data agree generally with the apparently scattered data reported by Ollett and Parker [24]. However, our data show that the viscosity of the fresh melt changes suddenly at 367 K where the melt relaxes: the viscosities of the relaxed melts are systematically about a half-order of magnitude lower than that of the fresh melt.

This means that, in a narrow T range around 367 K, the viscosity of a fresh fructose melt is time-dependent. Isothermal viscosity relaxations at 367.2 and 371 K are shown in Fig. 12. The initial viscosities ($\eta(0)$) marked on the graph were obtained by the extrapolation of the low-temperature viscosities shown in Fig. 13. The viscosity decreases in these isothermal relaxation processes are qualitatively what might be expected from the isothermal increases in entropy observed calorimetrically, as will be discussed. Again, the isothermal viscosity relaxation is not a simple exponential process. Again also, decomposition of the melts is not a factor in the isothermal viscosity relaxation. Further, it was our direct observation that the equilibrium

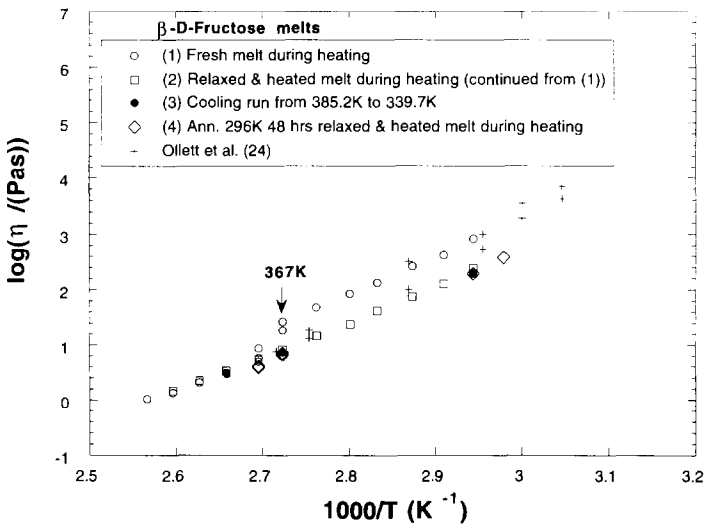

Fig. 11. Shear viscosities of β-D-fructose showing the displacement in the melt viscosity which follows annealing in the vicinity of 370 K. Comparison is made with data from Ref. [24].

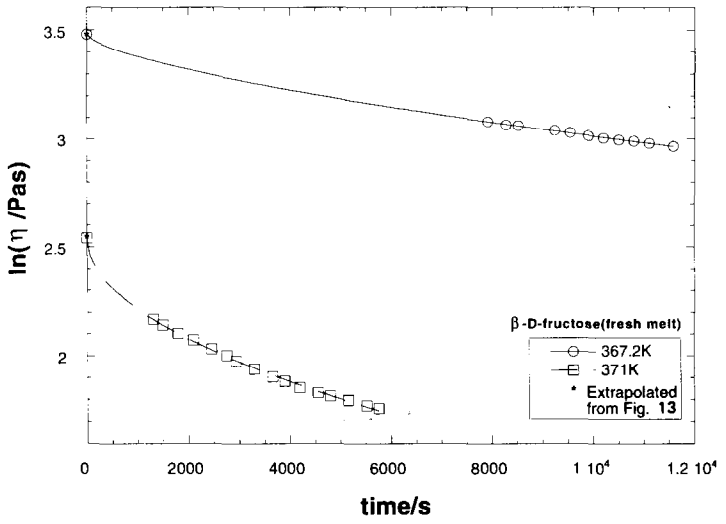

Fig. 12. Isothermal decreases in shear viscosity which occur in the same temperature range where enthalpy relaxation occurs; points at origin are from extrapolation of unrelaxed melt data from lower temperatures.

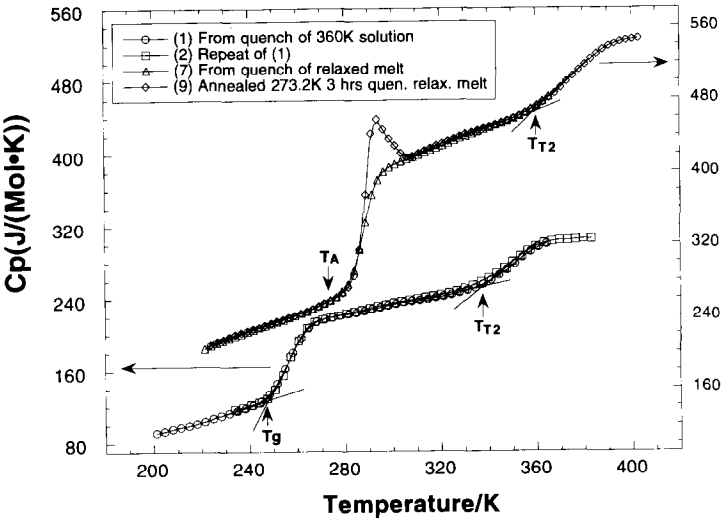

Fig. 13. DSC scans of heat capacity of hydrated melt of β-D-fructose containing 0.47 mole fraction of H_2O, showing the presence of the T_1 anomaly shifted down in temperature proportionally to the T_g decrease. Comparison is made with C_p of the anhydrous melt both before and after annealing.

viscosity showed on change when the melt was annealed at 373 K, and even above at which the decomposition proceeded relatively rapidly according to 13C NMR results (see discussion).

When a relaxed melt is annealed at a lower temperature, 296 K, for 48 h and then restudied isothermally at 367 K, it again shows time-dependent behavior, evidently having recovered a proportion of the slowly-relaxing species.

3.5. Hydrated melts

3.5.1. Heat capacities and EB transitions

To show that the EB transitions seen in the pure fructose and galactose melts are not unique to pure sugars, we show the behavior of some hydrated melts in Figs. 13 and 14. Fig. 13 shows, for instance, the heat capacity of a melt which is 0.47 mole fraction H_2O, 0.53 mole fraction β-D-fructose, and compares it with those of the quenched relaxed melt. It is noted that the glass transition temperature ($T_g = \sim 246.3$ K, $\Delta C_p = 80$ J mol^{-1} K^{-1}, the smeared-out T_{T_1}, and T_{T_2} (336 K, $\Delta C_p = 46.8$ J mol^{-1} K^{-1}) of this hydrated melt are all lower in temperature than those observed for the quenched relaxed melt of β-D-furctose, but otherwise are very similar. The solution exhibits the same annealing effects effects on T_g and on the EBT2 transition temperature as in the anhydrous systems.

3.5.2. T_g in relation to water content.

The values of T_g for several sugars with different water contents from the present and previous works are shown in Fig. 14. T_g values were determined at the onset point of the C_p increase in the present work, but by the midpoint of the C_p rise for galactose [25] and the blend of 0.124 fructose:0.876 sucrose [26]. The latter point lies about 10 K above the former and this adjustment has been made to avoid confusion. The insert in Fig. 14 shows T_g vs. water content in wt% rather than mol%, which changes the form considerably.

4. Discussion

The newest and most significant observations of this study are probably the irreversible slow relaxations which have been observed in the temperature range just below the temperature of initial fusion, 378 K (Figs. 10 and 12). These show that the liquid obtained in the initial fusion is in a non-equilibrium state, which is due to the fact that the product of initial fusion contains more of the β-pyranose tautomer (which makes up the crystal) than does the melt of lowest free energy.

Attainment of the equilibrium distribution is evidently a slow process relative to fusion by heat transfer across the crystal/liquid interface. The equilibrium melting point should, in this case, lie at a lower temperature than the crystallization onset temperature. However, at any lower temperature both the equilibration (conversion of β-pyranose form to other conformers) and the rate of diffusion of β- pyranose (formed at the crystal–liquid interface) into the more equilibrated melt at a distance from the interface, will be even slower. Hence, observing a true equilibrium fusion process, e.g., by placing a fructose crystal into an equilibrated melt [27], is probably not possible.

Part of the complexity of the molten state of fructose (and of galactose) is due to this initial non-equilibrium state obtained on fusion. Another part comes from the consequence of decomposition processes which set in around the melting point (but which fortunately occur on a time-scale longer than that of the equilibration). The final and, to us, the most interesting part of the complexity comes from the fact that the equilibrium

state of the liquid itself is temperature-dependent, with widely different time scales for equilibration with respect to its different degrees of freedom. In this discussion we will make an initial attempt to untangle these different sources of complexity and to provide a plausible account of the main phenomena observed both in present and in the previous studies.

Previous observers of the most prominent high temperature relaxation, T_2, have interpreted it differently at different times. For example, it has been interpreted as the glass transition for this substance [10], or as the galss transition for separable components of effectively a two-fluid melt [10]. While both ideas are partially correct, we think a one-component one-fluid model in which the constituent molecules have internal degrees of freedom which are accessible at melting temperatures and which influence the coupling of molecules to their neighbours, is more accurate and satisfying. We now discuss the sources of complexity in molten fructose in the order decomposition, initial equilibration, and temperature-dependent equilibration.

4.1. *Effects of decomposition*

The effects of decomposition are the least studied in the present work, and our principal concern is to ensure that they do not confuse our search for clarification of the interesting behaviour of pure fructose (and galactose). In this respect it is fortunate that, according to the ^{13}C NMR, shown in Fig. 2, decomposition can be almost completely avoided if temperatures above that of the initial melting point (378 K) are avoided for times greater than a few minutes, since even 374 K for six hours showed minimal development of new NMR peaks.

The effects of decomposition generally seems to be to decrease T_g and decrease the strength of T_2. Dehydration alone should not affect T_g much since it can be argued that the effects of plasticization by released water should almost quantitatively be canceled by T_g increases from the larger two-ring anhydrite molecule. The decreases observed must come from the many small-molecule fragmentation products [13].

4.2. *Tautomerization and the initial melt equilibration process*

The time-dependent changes in enthalpy and viscosity observed around 365–371 K in this work are surely due to slow equilibration amongst the tautomeric forms of the β-D-fructose molecules which in the crystal are all in the β-pyranose form (six-membered ring, see Fig. 1). While this latter is the lowest energy form, differing from the next lowest energy form, β-furanose, by $\approx 27\,kJ\,mol^{-1}$ [16], it only constitutes 70% of the molecules in a D_2O solution at 303 K, or 60% of a fresh fructose melt at 378 K. Clearly, the entropy of mixing favors the presence of more energetic forms. Tautomerization of sugar molecules in both protic and aprotic solution media has been extensively studied [28–32]. Not only are the proportions of tautomers and their enthalpy differences well known, but the tautomerization rates have also been measured [8, 28–32]. The generally accepted [8] sequence of rates is

α-furanose <=> β-furanose > pyranose <=> furanose
> α-furanose <=> β-furanose

We abbreviate these as α-f <=> β-f, and so on. The enthalpy absorbed in the equilibration process at 373.8 K seen in Fig. 10 amounts to 13.9 kJ mol^{-1}, and corresponds to the part of the total process that was left after fusion at 378 K, and temperature equilibration at 373.8 K. It somewhat exceeds the enthalpy of β-p → β-f, which was unexpected, and is about 45% of the enthalpy of fusion 29.8 kJ (a non-equilibrium enthalpy change).

We note here that this change is at least qualitatively compatible with the observed viscosity changes. According to the Adam–Gibbs entropy theory of relaxation [33], an increase in entropy associated with configurations should lead to a decrease in viscosity changes. According to the Adam–Gibbs entropy theory of relaxation [33], an increase in entropy associated with configurations should lead to a decrease in viscosity according to

$$\eta = \eta_0 \exp(C/TS_c) \tag{1}$$

where η_0 and C are constants and S_c is the configurational entropy (approximately ΔS_F at the melting point). Since the liquid entropy increases as heat is absorbed on holding at 375 K, the decrease in viscosity observed is in the expected direction. A decrease in viscosity would also be expected from the changes in H-bonding implied by the β-p → β-f structural change since the β-pyranose arrangement in the crystal provides a 3-dimensionally extensive H-bond net. Consistent with these considerations is also the fact that the proportion of the entropy of fusion which remains in the glass below T_g (not discussed further here) is considerably greater in fructose and galactose (fresh melts) than it is in the case of sucrose which has no liquid state anomalies.

4.3. *Tautomerizations and heat capacity anomalies*

Having once observed that the tautomer equilibration is slow, further anomalies in heat capacities are to be expected. Even in the absence of slow equilibration, heat capacity anomalies would be expected to appear if reversible changes in structural isomer concentrations can occur in the liquid range. Such equilibria should give rise to distinct two-state heat capacity contributions to to total observed quantity. These have been extensively discussed in connection with interpretation of the glass transition itself [34–36], for which they prove instructive, though usually unsatisfactory [36].

$$A \Leftrightarrow B \tag{2(a)}$$

with changes in thermodynamic quantities, ΔH, ΔV, ΔS

$$H = X_A H_A + X_B H = H_A + X_B \Delta H \tag{2(b)}$$

since

$$X_B = 1 - X_A \tag{2(c)}$$

so

$$C_p = [\partial H/\partial T]_p = R(\Delta H/RT)^2 N_B(1 - N_B) \tag{2(d)}$$

where

$$N_B = \{1 + \exp[(\Delta H - T\Delta S/RT]\}^{-1} \quad 2(e)$$

When ΔS is zero, this heat capacity increment is small at all temperatures, and maximizes at 3.76 J mol^{-1} K^{-1} (Schottky anomaly) at a temperature determined by ΔH. IF ΔS is large, however, the whole process is compressed in temperature, and the heat capacity at the maximum, which appears then at a lower temperature, can be large [36, 37]. When there are several possible two-state exchanges, there may be the same number of anomalies to be seen. Their strengths will depend not only on the ΔS value, but also on the mole fraction of tautomer free to participate. Of the possible equilibria mentioned above, only those involving p–f conversions have ΔH values sufficient to appear in the temperature range of the present anomalies, and the entropy change would have to be very large to account for the magnitude of the C_p jump. The relations between ΔH, and ΔS values and the temperature and magnitude of the C_p maximum are given in Ref. [36], Fig. 3.

Based on the population factors alone (see Table 1), the most prominent one would be the β-pyranose $\Leftrightarrow$ β-furanose exchange. For ΔH about 12 kJ mol^{-1}, the excess C_p would maximize only at 700 K, but a DS value of 30 J mol^{-1} K^{-1} would drop the T_{max} to below 400 K, and raise the $C_{p,max}$ into the range observed. Then, in the viscous medium, the crossing of the barrier between the two states might be impeded, and a fraction of the "excited state" (species B) molecules surviving at the lower temperature during cooling, could then become kinetically trapped in the B state, and ergodicity would be broken for lower temperatures. The less prominent αp–βf and αp–αf exchanges could account for the weaker T_1 and T_3 anomalies.

The presence of non-ergodic states is definitively indicated by the results of annealing experiments, in which the system is annealed below the EB temperature. During the annealing time the system slowly loses B species population, and hence enthalpy, as it approaches the equilibrium state. Then on subsequent upscanning at the normal rate, the extra lost enthalpy is regained in a narrow range of temperatures where the re-equilibration time becomes commensurate with the scanning rate, as is well-known in glass transition phenomenonology.

This overshoot effect is seen for T_2 in Fig. 6, though there are important differences between the T_2 behavior in Fig. 6 and that seen at the normal glass transition. In the latter, the lower the annealing temperature the higher the temperature of the subsequent heat capacity jump and the greater the overshoot [38]. In the T_2 case, the anomaly moves down in temperature as the annealing temperature is lowered. This effect could be due to the fact that the state of tautomer equilibrium does not directly control the relaxation time at the glass transition, and is in fact only weakly coupled to it. However, it could also be related to decomposition effects in view of the heating limit being set too high (410 K) in this series. We will not attempt further analysis of this effect until further measurements have been made. Decomposition of the melt may also be responsible for another troubling aspect of the observation, namely the magnitude of the high-temperature heat capacity decreases with increasing run number. While this would imply a lack of reversibility, it agrees with the observation of Finegold et al. [9]

that the C_p anomaly becomes weaker with increasing heating time (compare run 1 and run 14 in Fig. 6, both of which are made by quenches of the melt).

Following the above discussion, it must be recognized that we do not have much evidence that the two weaker transitions T_1 and T_3 involve ergodicity breaking: they could well be entropy-enhanced Schottky anomalies due to tautomer exchanges which remain in equilibrium at all times. Further work will need to be done to resolve these issues.

To assist the discussion we relate, in Fig. 14, the time scales we have measured for the slow enthalpy and viscosity relaxations to the shear relaxation times derived from the viscosity data by means of the Maxwell equation

$$\eta = G_\infty \tau_s \tag{3}$$

with reasonable values for G_∞. It is interesting then to put on the diagram the relaxation times for the T_2 process based on the notion that when a process begins to come back into equilibrium from the non-ergodic state during a DSC scan at 10 K min^{-1}, the relaxation time of the process is 10^2 s. Using data from the scans of Fig. 6 and 7 at 10 K min^{-1} and other rates, we obtain the points denoted f–p in Fig. 15. Rather than falling on the line of slow enthalpy and viscosity relaxation times as might have been expected, they fall at somewhat shorter times and exhibit a different slope. It is not clear to us at this time whether this difference reflects our lack of understanding of the phenomenology or a non-simple relation between the source of the isothermal relaxations and the source of the slow degree of freedom responsible for the heat capacity jump.

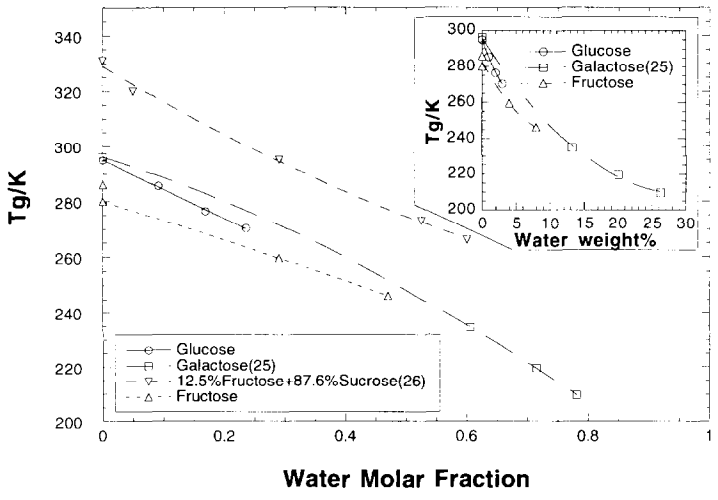

Fig. 14. Variation of T_g with water content for glucose, galactose and fructose melts, and of one blend. Insert shows data for compositions in wt% water.

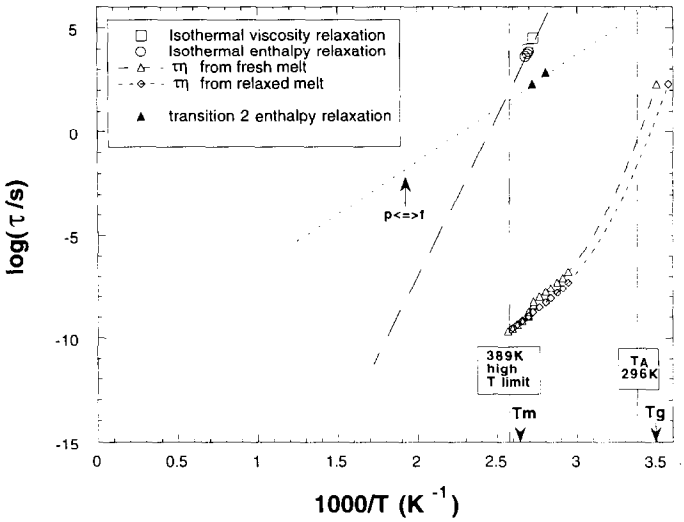

Fig. 15. Comparison of relaxation times of slow liquid state processes with shear relaxation times for fresh melts and relaxed melts.

5. Concluding remark

A full understanding of these complex systems will require further structural studies. The systems would be good candidates for the sort of chronophotometry studies reported earlier [4], except that the present systems would then require use of IR spectroscopy.

References

[1] M. Cukiermann and D.R. Uhlmann, J. Non-Cryst. Solids, 12 (1973) 199.
[2] C.A. Angell and D.L. Smith, J. Phys. Chem., 86 (1982) 3845.
[3] C.A. Angell, P.H. Poole and J. Shao, Nuovo Cimento (in press). C.A. Angell, Science, March 31 issue (1995).
[4] C.A. Angell, J. Green, D. List, Z. Qing, H. Snapati and J.C. Tucker, in W. Kinser and R.A. Weeks (Eds.), Proc. Nashville Conference on Effect of Modes of Formation on Glass Structure and Properties, Diffusion and Defect Data, 53–54 (1987) 77.
[5] D.L. Smith, (unpublished work).
[6] Jain
[7] The possibility of studying the problem of Al–Si distributions in glassy alumino-silicates of different thermal histories has only recently become feasible through solid state NMR spectroscopy. (P.F. McMillan and J. Stebbins).
[8] F. Franks, Pure Appl. Chem., 59 (1987) 1189–1202.
[9] L. Finegold, F. Franks and R.H.M. Hatley, J. Chem. Soc., Faraday Trans. 1, 85(9) (1989) 2945–2951.
[10] L. Slade and H. Levine, Pure Appl. Chem., 60 (1988) 1841–1864.
[11] P. Tomasik, Adv. Carbohydr. Chem. Biochem., 47 (1989) 203.

[12] R.S. Shallenberger and G.G. Birch, Sugar Chemistry, Westport, Connecticut, The AVI Publ. Co., Inc., (1975), Ch. 7, pp. 169–193.
[13] M.L. Wolfrom, W.W. Binkely, W.L. Shilling and H.W. Hilton, J. Am. Chem. Soc., 73 (1951) 3553–3557.
M.L. Wolfrom and W.L. Shilling, J. Am. Chem. Soc., 73 (1951) 3557.
M.L. Wolfrom and M.G. Blair, J. Am. Chem. Soc., 70 (1948) 2406–2409.
[14] D.A. Ditmars and T.B. Douglas, J. Res. Natl. Bur. Stand. Ser. A, 75A (1971) 401–420.
[15] S.S. Chang and A.B. Bestul, J. Chem. Phys. D, 56 (1972) 503–516.
[16] D.J. Nicole, B. Gillet, E.N. Eppiger and J-J. Delpuech, Tetrahedron Lett., 23 (1986) 1669–1672.
[17] R. Kuhn and F. Haber, Chem. Ber., 86 (1953) 722.
[18] T.C. Crawford, G.C. Andrews, H. Faubl and G.N. Chumurny, J. Am. Chem. Soc., 102 (1980) 2220–2225.
[19] D. Horton and Z. Walaszek, Carbohydr. Res., 105 (1982) 145–153.
[20] K. Bock and C. Pederson, Adv. Carbohydr. Chem. Biochem., 41 (1983) 27–66.
[21] E.W. Nelson and R.F. Newton, J. Am. Chem. Soc., 63 (1941) 2178.
[22] F. Kawaizumi, S. Kushida and Y. Miyahara, Bull. Chem. Soc. Jpn., 54 (1981) 2282–2285.
[23] G. Blond and D. Simatos, Thermochim. Acta, 175 (1991) 239–247.
[24] A.L. Ollett and R. Parker, J. Texture Studies, 21 (1990) 355–362.
[25] D. Simatos, G. Blond and M. LeMeste, Cryo-Letters, 70 (1989) 77–84.
[26] T. Soesanto and M.C. Williams, J. Phys. Chem., 85 (1981) 3338–3341.
[27] An attempt at this experiment was made and only a smeared out endothermic process, commencing at ~ 99 K, was observed. Nevertheless, the fact that heat absorption commenced at a much lower temperature than when the "dry" crystal commences to melt, proves our point.
[28] S.J. Angyal, Adv. Carbohydr. Chem. Biochem., 42 (1982) 15–68.
[29] C.J. Moye, Adv. Carbohydr. Chem. Biochem., 27 (1972) 85–125.
[30] J.R. Snyder, E.R. Johnston and A.S. Serianni, J. Am. Chem. Soc., 111 (1989) 2681–2687.
[31] T.E. Acree, R.S. Shallenberger and L.R. Mattick, Carbohyd. Res., 61 (1968) 498–502.
[32] M.A. Kabayama, D. Patterson and L. Piche, Can. J. Chem., 36 (1958) 557.
J.M. Sturtevant, J. Phys. Chem., 45 (1941) 127.
[33] G. Adam and J.H. Gibbs, J. Chem. Phys., 43 (1965) 139.
[34] P.B. Macedo, W. Cappo and T.A. Litovitz, J. Chem. Phys., 44 (1966) 3357.
[35] C.A. Angell and J. Wong, J. Chem. Phys., 53 (1970) 2053.
[36] C.A. Angell and K.J. Rao, J. Chem. Phys., 57 (1972) 470.
[37] If ΔS is very large, the whole enthalpy gain can be compresed into a very narrow temperature range and the exchange can look like a first-order transition, as in the case of the denaturing transition of proteins.
[38] I.M. Hodge, Macromolecules, 20 (1987) 2897.